Applied Surface Science 406 (2017) 144–149

Contents lists available at ScienceDirect

Applied Surface Science

journal homepage: www.elsevier.com/locate/apsusc

Full Length Article

Angle resolved XPS for selective characterization of internal and external surface of porous silicon

Anna Lion[a,1], Nadhira Laidani[b], Paolo Bettotti[a], Chiara Piotto[a], Giancarlo Pepponi[c], Mario Barozzi[c], Marina Scarpa[a,*]

[a] Nanoscience Laboratory, Department of Physics, University of Trento, Via Sommarive 14, 38123 Povo, Trento, Italy
[b] Centre for Materials and Microsystems, Bruno Kessler Foundation, Via Sommarive 18, 38123 Povo, Trento, Italy
[c] Micro Nano Facility, Bruno Kessler Foundation, Via Sommarive 18, 38123 Povo, Trento, Italy

ARTICLE INFO

Article history:
Received 11 January 2017
Received in revised form 8 February 2017
Accepted 13 February 2017
Available online 16 February 2017

Keywords:
Porous silicon
Porous silicon microparticles
Space selective functionalization
Angle resolved XPS
Surface hydrophilicity
Hydrophobic cavities

ABSTRACT

Selective functionalization of the external/internal pore surface of porous silicon is of interest for the numerous potential applications of this material, in particular in pharmacology. With the aim of obtaining porous silicon platforms compatible with the aqueous environment and providing hydrophobic pores to load poorly water soluble molecules, we set-up a three step functionalization procedure consisting in two hydrosilylation reactions separated by the selective etching of the external surface. This procedure was applied both, to porous layers and porous microparticles. The characterization of the functionalized material by conventional techniques such as contact angle and FTIR showed a change of the properties of porous structures in line with the expected surface modifications. However, these techniques do not permit to clearly distinguish between internally and externally grafted functional groups. For this reason, an innovative procedure based on angle-resolved XPS was set-up and applied to differently functionalized pSi layers. By this technique, we obtained indications of prevalent grafting of hydrophilic moieties on the external surface and hydrophobic ones inside the pores.

1. Introduction[2]

Interface-mediated processes play a fundamental role in determining the interaction of porous materials with the surrounding environment, [1]. These interactions are furtherly enhanced when nanosize combines with porosity and are in part responsible of peculiar properties of nanostructured porous materials in catalysis, storage and sensing [2,3]. In some cases, the confinement of molecules into specific regions through spatially selective chemical modification of the pore surface is required to fully exploit the properties of the porous framework. Many promising approaches have been suggested, however, up to now, only few successful cases of selective functionalization of inner/outer porous structures have been achieved [4,5]. This is in large part due to the difficult implementation of selective chemical modifications on either, the outer sample or the inner pore surfaces. The second non-trivial problem is the mapping of the line profile of the surface inside the pores, in particular if a gradient of the grafted chemical groups is expected. In fact, the most sophisticated techniques lack of the necessary resolution [6] or do not provide information about the chemical functional groups of organic carbon [7,8]. Finally, the techniques based on progressive surface etching do not provide reliable composition of surface organic monolayers grafted on a porous substrate, due to the variable etching rate of a porous structure and to the mixing of the atoms within the samples [9,10].

Silicon is a substrate suitable for fabrication of versatile porous materials with easy tunability of pore size and shape, which find applications for storage and delivery of drugs, microfluidics and flow-through sensors [11]. In these applications, the inner pore surface should expose chemical moieties with specific properties, such as low non-specific absorption of analytes flowing inside (in flow-through sensors) [12], variable fluid flow rate (in microfluidics) [13], high affinity for the loaded molecules and tunable release rates (in drug delivery or storage of matter) [14,15]. Conversely, the outer surface should provide affinity to, and protection from, the surrounding environment [16]. A large spectrum of functionalization routes of porous silicon (pSi) has been reported [17] among which the hydrosilylation reaction induced by heat, UV or

* Corresponding author.
E-mail addresses: marina.scarpa@unitn.it, marina.scarpabertolo@gmail.com (M. Scarpa).
[1] Present address: Faculty of Science, University of Nottingham, Nottingham UK.
[2] Abbreviations: pSi, porous silicon; pSi-particles, porous silicon microparticles; TOA, take-off angle.

http://dx.doi.org/10.1016/j.apsusc.2017.02.099
0169-4332/

visible light [18] which allows the introduction of hydrophilic or hydrophobic organic coating. Alternatively, oxidation produces a hydrophilic inorganic surface suitable for interaction with aqueous environments [19]. The chemical versatility of pSi surface makes this material a good platform to test spatially selective functionalization routes. In this regard, Kilian et al. [20] proposed a simple approach to obtain a selective modification of inner and outer silicon pore surface. Their strategy consists in the combination of surface tension and capillarity to regulate the entrance of reactive solutes inside the pores. Based on the same principle, Wu and Sailor [21] proposed the use of two immiscible liquids, one inert and the other chemically reactive with pSi. The inert liquid infiltrates the nanopores protecting them from the reactive one which modifies only the external surface. By the proposed procedure, hydrophilic pores and hydrophobic organic coating on the external surface are expected [21,22]. This selective coating is suitable for water confinement inside the pores but not for the preparation of stable colloidal suspension of pSi microparticles (pSi-particles) for the delivery of drugs through biological fluids. In this case, the pSi-particles must travel in aqueous environment and transport poorly soluble molecules. Here, for these systems, we propose a simple functionalization approach which provides hydrophobization of the inner pore walls, while the exposed surface is grafted with hydrophilic groups. Bulk porous silicon samples were used to enlighten about the difference between the external surface and the pore walls. We show that XPS at variable take-off angle (TOA) is a method to investigate compositional differences between the surface inside and outside the pores of pSi. The approximations and the limits of this approach have been evaluated and discussed also in the light of its possible application to other ordered porous materials. Since the pSi-particles are ideal drug carriers as they conveniently interact with various biological environments to release drugs with predefined dynamics [23,24], whenever possible the characterization tests were performed also on this material.

2. Experimentals

2.1. Reagents

Anhydrous toluene (purity >99.8%) was purchased by Alfa-Aesar (Milan, Italy). All the other reagents were of the highest available purity and were purchased by Sigma Aldrich (Milan, Italy).

2.2. pSi and pSi-particles production

Two groups of porous Si samples were utilized to perform the present investigation: porous Si grown over bulk silicon (pSi) and porous Si microparticles (pSi-particles) obtained from pSi by sonication. pSi was used to characterize the functionalization procedures described later on, in terms of contact angle (CA) and profile of the grafted groups by XPS. A complete set of FTIR characterization data was obtained both for pSi and pSi-particles.

pSi was obtained by electrochemical etching of crystalline silicon, performing constant current anodization in alcoholic HF solutions. Two types of pSi have been prepared: pSi-1 and pSi-2. pSi-1 was obtained using antimony doped, resistivity 0.01 ohm cm, ⟨100⟩ oriented crystalline silicon and applying a current density of 30 mA cm^{-2} for 15 min in HF 16% hydro alcoholic etching solution.

pSi-2 was obtained using antimony doped, resistivity 0.3-0.5 ohm cm, ⟨100⟩ oriented crystalline silicon and applying 105 mA cm^{-2} current density for 15 min in HF 16% hydro alcoholic etching solution. In particular, these latter samples were used to characterize the surface functionalization with XPS by exploiting the greater signal obtained from larger pores during the depth profiling. The etched samples were rinsed in absolute ethanol and dried by a gentle nitrogen flow.

pSi-particles were obtained from both, pSi-1 and pSi-2, however the functionalization experiments reported later on refer to pSi-particles obtained from pSi-1. pSi-particles were obtained by gentle scratching the pSi with a cutter. The powder was collected, suspended in anhydrous toluene saturated with nitrogen and sonicated at 400 W for 5 min.

2.3. Functionalization of the pSi samples

2.3.1. First step: hydrosilylation reaction by alkenes

pSi and pSi-particles (16 mg mL^{-1}) were suspended in anhydrous toluene containing 1.6 mM alkene (heptene or 11-Br 1-undecene) at RT, under nitrogen atmosphere. The reaction solution was stirred for two hours and illuminated by a Visible led lamp (250 W) and a 365 nm UV led lamp (100 W). We used the simultaneous UV and Visible illumination to allow both, the exciton-mediated and radical-induced reaction pathways [18]. pSi was rinsed 5 times with pentane and dried by a gentle nitrogen flow, while the pSi-particle suspension was transferred in glass tubes and centrifuged for 15 min at 150*g*. The supernatant was discarded, the powder re-suspended in pentane and centrifuged again. This step was repeated 5 times. The obtained samples were referred to as alkyl-pSi or alkyl-pSi-particles.

2.3.2. Second step: infiltration with pentane and etching in diluted aqueous HF

Dried alkyl-pSi was immersed in pentane for 30 min then transferred in HF (0.1–2%) for 1 min. The sample was rinsed with ethanol and dried by a nitrogen flow. Alkyl-pSi-particles were infiltrated and etched by the same procedure, except that the incubation in HF lasted for 30 s, then the micro powder was centrifuged at 16000*g* for 30 s and rinsed in ethanol 5 times. The obtained samples were referred to as etched-pSi and etched-pSi-particles.

2.3.3. Third step: hydrosilylation reaction by acrylic acid

The etched-pSi and etched-pSi-particles were transferred in toluene containing 50 mM acrylic acid and left to react at RT for two hours under nitrogen flow and gentle stirring. Visible and UV illumination were used as for the first hydrosilylation reaction.

The samples were rinsed in ethanol and referred to as propionic-pSi and propionic-pSi-particles.

2.4. FTIR, SEM, contact angle and XPS analysis

The chemical groups present on pSi and pSi-particles were investigated by Fourier Transform Infra-Red (FTIR). The infrared spectra were acquired by using a micro-FTIR Nicolet iN10 instrument, in the spectral range of 500–4000 cm^{-1} with 4 cm^{-1} resolution. The pSi samples were analyzed in reflectance mode, the pSi-particle suspensions were deposited on a ZnSe slab, left to dry under gentle nitrogen flow and analyzed in transmission mode.

SEM analysis were performed on a Jeol JSM-7401F.

Contact angles (CA) were measured on pSi by a home-made apparatus equipped with a digital camera coupled to an optical zoom. The images were collected using the software Motic images Plus 2.0 and analyzed by the software ImageJ.

pSi was analyzed by Angle-resolved X-ray photoelectron spectroscopy (AR-XPS) with a Scienta ESCA 200 instrument using monochromatized Al Kα radiation at 1486.6 eV. Wide scan surveys and resolved spectra for C1s, Si 2p, O1 s and Br2d core levels were recorded. All binding energies are referenced to the Fermi level (E_F). Shirley-type background subtraction was applied to the core levels peaks and the latter were curve fitted using Gaussian shape single peaks. The binding energy scale was calibrated assuming the

Table 1
Structural features of the pSi.

pSi	pSi-1	pSi-2
Average pore diameter (nm)	10	250
Average pores distance (nm)	20	500
Pore length (μm)	5	12
Porosity (%)	80	50

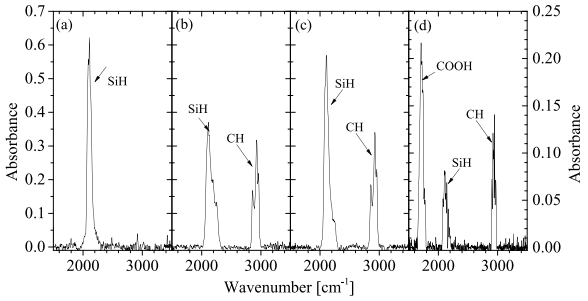

Fig. 1. FTIR spectra of pSi-particles treated with different chemical moieties.
a) pristine pSi-particles; b) alkyl-pSi-particles; c) alkyl-pSi-particles infiltrated by pentane and etched in 1% HF; d) propionic acid-pSi-particles. The pSi-particles were obtained from pSi-1, the first functionalization step was performed by heptene. Left Absorbance scale for spectra a–c), right for spectrum d).

Table 2
Static contact angle of water on pSi-1 samples.

Sample type	Left angle	Right angle	Mean angle
A	125 ± 1	124 ± 1	125 ± 1
B	120 ± 2	118 ± 1	119 ± 2
C	124 ± 1	121 ± 1	123 ± 2
D	72 ± 2	71 ± 2	72 ± 2

A) pristine pSi-1; B) alkyl-pSi-1; C) etched-pSi-1 (etching in 1% HF); D) propionic –pSi-1.
The first functionalization step was performed by using heptene.

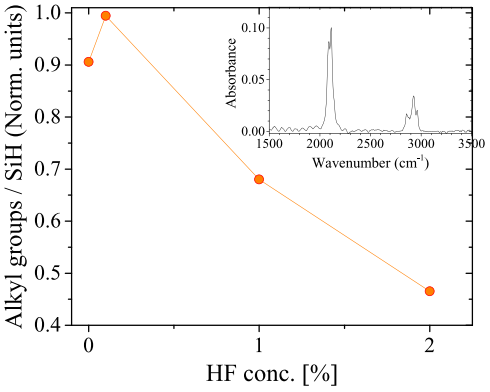

Fig. 2. Surface chemical composition of the etched alkyl-pSi-particles as function of HF concentration in the etchant solution.
The pSi-particles were obtained from pSi-1 layers, the first functionalization step was performed by heptene. Alkyl-pSi-particles were infiltrated with pentane and exposed to etchant solutions containing variable HF concentration for 1 min. The chemical composition was expressed as the ratio between the sum of the areas of the alkyl peaks at 2800–3000 cm^{-1} and the SiH peak at 2250 cm^{-1} (two representative peaks are shown in the inset). Similar results were obtained when the same experiment was performed on layers of alkyl-pSi instead that on alkyl-pSi-particles.

binding energy of Ag 3d line at 386.16 eV with respect to E_F. The chemical composition were derived by applying Scienta sensitivity factors for the core levels. No special surface treatment such as ion etching in the analysis apparatus was carried out before the spectra acquisition. In order to define the depth variation of the surface chemical composition, the electron take-off angle (TOA) was varied from *90°* to *20°* with respect to the surface. The lower the TOA value, the shallower the analysis region.

3. Results and discussion

SEM analysis of the pSi samples with different resistivity (pSi-1 and pSi-2) revealed the structural features summarized in Table 1. Representative SEM images of pSi and of pSi-particles are reported in Fig. S1 and S2 in the Supporting Information (SI).

Selective coating of the outer and inner surface of the pSi samples was obtained by the three-step functionalization procedure. The first step consists in the introduction of a hydrophobic coating of the entire surface (internal and external) of the pSi-1 by alkylation with 1-heptene. In the case of pSi-2, 11-bromo-1-undecene was used as alkylating agent to detect the grafted hydrophobic molecules using the XPS features of bromine. Alkyl-pSi is obtained at the end of this step. In the second step, the pores of the alkyl functionalized pSi are infiltrated with pentane and suddenly immersed in aqueous HF. This diluted etchant solution removes few layers of the accessible silicon atoms together with their organic coating. Only the external surface is etched, since the pore walls are protected by pentane. The third step consists in a hydrosilylation reaction by acrylic acid which grafts mainly the just-etched external surface so that propionic groups are exposed on the external surface, while alkyl groups still cover the inner surface.

The chemical composition after each modification step was characterized by FTIR. Similar FTIR features were obtained for all the samples, independently of their morphology. Fig. 1 reports a typical FTIR spectrum with the main peak assignments. In particular, SiH functionalities are exposed on the surface of the pristine pSi-particles (peak at 2112 cm^{-1}, Fig. 1(a) [25]) and decrease after hydrosilylation by alkene (Fig. 1(b)) which introduces an alkyl monolayer on the surface accessible to the reactants. The vibration features in the spectral interval 2800–3000 cm^{-1} of Fig. 1(b) belong to the alkyl chains and deconvolution of these peaks and of the other relevant features lead to the spectral assignments of Table S1 reported in the SI [25–29]. The shoulder of the SiH vibration at about 2250 cm^{-1} in Fig. 1(b) is associated with the back oxidized SiH stretching [27] and indicates that some oxidation occurs during the functionalization step. This side reaction is confirmed also by the feature of silicon oxide at 1100 cm^{-1} (not shown in Fig. 1(b)). The surface hydrophobicity of heptyl-pSi was supported by a mean CA of 119 ± 2 measured over pSi layers, only slightly lower than the CA (125 ± 1°) measured for the pristine pSi (see Table 2). When heptyl-pSi-particles were infiltrated with pentane and immersed in HF (Fig. 1(c)) the SiH peak was partially restored which makes the surface still hydrophobic (as confirmed also by the large CA, see Table 2), meanwhile the FTIR features of the alkyl chain at 2800–3000 cm^{-1} decrease. The decrease of the ratio between the two peak areas (Alkyl groups/SiH) depends on HF concentration (as shown in Fig. 2). The semi-quantitative analysis of the surface coverage by the alkyl groups reported in Fig. 2 was obtained normalizing the FTIR peaks at 2800–3000 cm^{-1} assigned to alkyl groups [26] to the area of the SiH peak taken as internal reference for each sample. Since this normalized value represents the density of surface sites to which alkyl chains are grafted with respect to SiH sites still free, we used it to establish that the dipping in 1% HF for 1 min is sufficient to remove the exposed alkyl groups, as shown in Table 3. 1 min dipping for removing the surface layers of silicon is also in accord with published values of the etch rates of pSi in diluted HF solutions [30].

The propionic-pSi-particles obtained after hydrosilylation by acrylic acid of alkyl-pSi-particle previously infiltrated and etched in HF, showed the characteristic carboxyl stretching at 1720 cm^{-1} (Fig. 1D and Table S1) and the surface of pSi undergoing the same

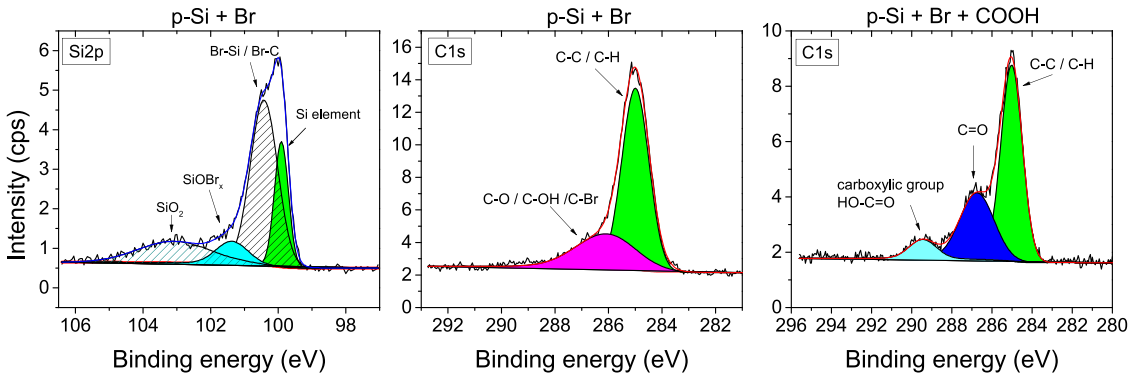

Fig. 3. XPS spectrum of pSi-2.
Left panel: Si2p components of alkyl-pSi-2. Central panel: C1s components of alkyl-pSi-2. Right panel: C1s components of propionic acid-pSi-2.
To obtain alkyl-pSi-2 the pSi-2 was functionalized by 11-bromo-1-undecene. To obtain propionic-acid pSi-2, the alkyl-pSi-2 was infiltrated with pentane, etched in 1% HF and functionalized by acrylic acid. The XPS spectra were acquired at grazing TOA.

Table 3
Removal of the alkyl chains by dipping in HF solutions at various concentrations.

alkyl groups/SiH%			
A	B	C	D
100	87	71	69

The ratio alkyl groups/SiH was calculated as the ratio between the peak area of the multiplet of peaks centered at 2934 cm^{-1} and that of the SiH peak centered at about 2106 cm^{-1}. This ratio was considered as 100% for heptyl pSi-particle. A) heptyl-pSi-particle; B) heptyl-pSi-particle infiltrated with pentane after 1 min dipping in 0.1% HF; C) dipping in 1% HF; D) dipping in 2% HF.

treatment turned to be hydrophilic with a mean CA of 72 ± 2 (see Table 2). In spite of the hydrophilicity, the alkyl chain peak intensity in Fig. 1D is remarkable, suggesting that the alkyl chains still cover the surface inside the pores and acrylic acid has been grafted on the external surface.

The penetration depth of microFTIR is of the order of several μm [31], thus, the whole volume of the pSi-particle samples was analyzed and we obtain a mean chemical composition of the samples. Conversely XPS is a surface-sensitive quantitative spectroscopic technique, since it investigates the surface-near layers up to a few nm thickness. To distinguish the contribution of the organic moieties on the external surface from that of the inner surface of the pores, we performed angle-resolved XPS measurements [32,33].

XPS spectra were acquired on pSi-2 samples, in which a specific hydrophobic probe was introduced during the first functionalization step. We used 11-Bromo-1-undecene instead of heptene as hydrophobic alkylating agent because Br is an excellent probe, since it offers the advantage of a low detection limit and high specificity due to the absence of Br contaminations. To probe the hydrophilic molecules grafted by the second functionalization step, we monitored the carboxyl component which is well distinguishable in the C1s XPS spectrum (see later on). To correct for the other parameters which affect the absolute signal intensity such as the sample morphology and the variable orientation of the sample with respect to the source and the detector, the intensities were normalized with respect to that of a suitable reference signal. The surface analysis was performed by varying the TOA between the direction of detection of photoelectrons and the sample surface. The details of the XPS experiment and of the data analysis are reported in the SI (section " XPS Experiment and data analysis" and Fig. S3). pSi samples are transparent to X-rays, conversely, the emitted photoelectrons are effectively captured by silicon (the attenuation length of silicon is 3.4 nm) [34]. Only the photoelectrons which pathway minimally interacts with the silicon skeleton are detected, so that, if the sample is tilted with respect to the detector, the surface of the pore wall is sampled until a definite pore depth (Fig. S3). This depth varies at variable TOA [35]: at increasing TOA, pores are sampled at larger depths.

In the limit case, when the uppermost surface of the layer is aligned with the detector direction (the grazing angle shown in the SI, Fig. S3c), mainly the organic over-layer on the external surface contributes to the signal. The limitations of the TOA-XPS approach to quantitative chemical surface analysis are discussed in the SI. However, the sources of uncertainties are minimized if chemical groups present in the organic over-layer are considered and the relative intensities of their signals at variable TOA are used to extract data about surface composition.

Fig. 3 (left panel) reports the Si2p signal of alkyl-pSi-2 with the four main components fitted (Si at 99.33, SiO_2 at 103.6, SiBr/SiC at 100.0 and SiOBr at 101.4 eV) [36]. The traces of bromine directly bound to silicon or silicon oxide indicates that, under UV irradiation, side reactions mediated by bromo radical occur [37]. The Br spectrum and the peak assignments [36,38,39] are shown in the SI (Fig. S4). Fig. 3 shows also the experimental spectrum in the energy region of C1 s of alkyl-pSi-2 (central panel) and of propionic-pSi-2 (right panel). The single components of the C1 s spectra were de-convoluted and centered at the typical binding energies of C—C/C—H, C═O/C—O—C/C—OH, and O—C═O. The fitting procedure converge to binding energies of 285.00, 286.10, 289.43 eV, in good agreement with the expected values [40]. It must be remarked that the carboxyl signal at 289.43 eV was detected in the propionic-pSi-2 only (right panel of Fig. 3), and was absent in the C1 s spectra of alkyl-pSi-2 (central panel of Fig. 3) and of pristine pSi-2 (not shown here). For this reason the peak at 289.43 is a reliable marker of propionic group introduced by the third functionalization step. All the spectra shown in Fig. 3 were obtained with a grazing TOA, at which prevalently the surface outside the pores is probed.

The homogeneous grafting of the alkyl chains in the whole Br-undecenyl-pSi-2 surface was verified by taking the XPS spectra at 90° TOA, at which both, the external and the internal pore surface, contribute to the detected signal, and at 40° TOA, angle at which the contribution of the photoelectrons emitted from the external surface weights more than at 90°. The ratio between the area of the bromine signal and the underlying silicon remains nearly constant at 90° and 40° (0.17 and 0.14 respectively) as shown in Fig. 4. Conversely, the same ratio measured for etched-pSi sample is TOA dependent, showing the lowest value at the grazing angle (Fig. 4). It should be remarked that the ratio $[Br]/[\Sigma[Si] \approx 0.05$ at the grazing angle, corresponds to a bromine peak disappearing into noise. This datum confirms that the removal of the alkyl chains from the external surface of alkyl-pSi by 1 min etching in 1% HF was almost complete. The data of Fig. 4 support also the hypothesis of

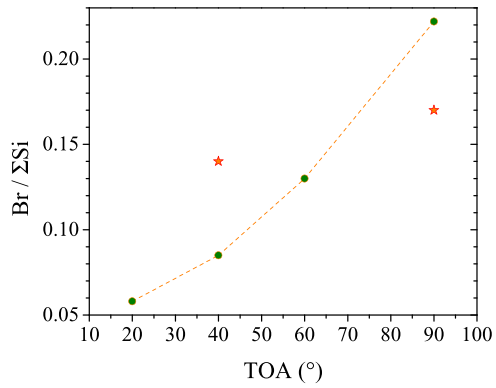

Fig. 4. Comparison of Br distribution before and after etching.
XPS spectra were obtained at variable TOA on alkyl-pSi-2 (stars) and etched-pSi-2 (circles). The area of the Si peak (sum of all the Si containing species) at each TOA value was taken as reference. 11-Bromo-1-undecene was used as alkylating agent.

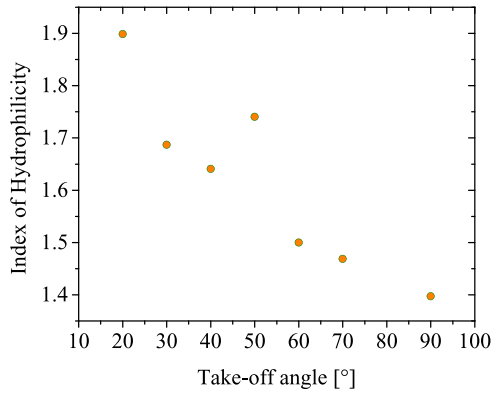

Fig. 5. Index of hydrophilicity *versus* TOA.
The sample was propionic-pSi2. 11-Bromo-1-undecene was used as alkylating agent for the first functionalization step. The index of hydrophilicity was calculated as the ratio between the area of the COOH peak of the C1s spectrum and the area of the Br3d spectrum.

uniformly grafted alkyl chains which are removed prevalently from the external surface by pentane infiltration and HF etching.

Because both, carboxylic group and bromine are present in the organic over-layer, the ratio of the areas of their peak is representative of the relative composition of the sampled surface, irrespectively of the geometric arrangement of the measurement. Because COOH and the alkyl chains to which Br is bound, heavily affect the surface wettability, we indicated the ratio between their peak areas as the "index of hydrophilicity". This index decreases at increasing TOA, as shown in Fig. 5, confirming that the surface is progressively more hydrophobic inside the pores. This is the first successful procedure to confine hydrophilicity on the external surface of pSi layers, preserving the hydrophobic environment inside the pore network. This confinement should allow a controlled passage of hydrophobic moieties entrapped inside the pores and the water exchange.

4. Conclusions

We demonstrated that two alkylation reactions spaced out by the selective etching of the outer surface, confine hydrophobic moieties inside pSi while the desired polarity is introduced on the outer surface. This functionalization procedure is a very general strategy, which can be applied to different material morphologies, such as porous layers or colloidal dispersion of porous microparticles, with pore diameter in the range 30–250 nm. This size versatility allows that the functionalized structures can be filled with hydrophobic molecules (i.e. to obtain drug delivery systems compatible with biological fluids) or apolar nanoparticles (i.e. to obtain nanocomposites for spintronics, magneto-optic devices, etc). By using an innovative analysis approach based on angle-resolved XPS, in combination with contact angle and FTIR spectroscopy, we provided experimental data on the distribution of the grafted organic groups along the pores of pSi films. As far as we know, this is the first report on the distribution of functional groups in a monolayer of organic molecules grafted on the external/internal surface of porous silicon. The prevalent confinement of hydrophilicity on the external surface and hydrophobicity inside the pores can be exploited for the control of nanofluidics over the interface of porous silicon devices, suggesting a further application of this functionalization strategy to porous silicon membranes.

Funding

This work was supported by the Italian Ministry of education [Grant number FIRB-RBFR12OO1G].

Acknowledgements

Marina Scarpa thanks Enrico Moser for his skillful assistance.

Appendix A. Supplementary data

Supplementary data associated with this article can be found, in the online version, at http://dx.doi.org/10.1016/j.apsusc.2017.02.099.

References

[1] M.E. Davis, Ordered porous materials for emerging applications, Nature 417 (2002) 813–821.
[2] T.-D. Nguyen, C.-T. Dinh, T.-O. Do, Tailoring the assembly interfaces, and porosity of nanostructures toward enhanced catalytic activity, Chem. Commun. 51 (2015) 624–635.
[3] Q. Chen, M. Luo, P. Hammershøj, D. Zhou, Y. Han, B. Wegge Laursen, C.-G. Yan, B.-H. Han, Microporous polycarbazole with high specific surface area for gas storage and separation, J. Am. Chem. Soc. 134 (2012) 6084–6087.
[4] C.M.A. Parlett, M.A. Isaacs, S.K. Beaumont, L.M. Bingham, N.S. Hondow, K. Wilson, A.F. Lee, Spatially orthogonal chemical functionalization of a hierarchical pore network for catalytic cascade reactions, Nature Mater. 15 (2016) 178–183.
[5] M. Pla-Roca, L. Isa, E. Kumar, Selective (bio)functionalization of solid-state nanopores, ACS Appl. Mater. Interfaces 7 (2015) 6030–6035.
[6] F. Meirer, D.T. Morris, S. Kalirai, Y. Liu, J.C. Andrews, B.M. Weckhuysen, Mapping metals incorporation of a whole single catalyst particle using element specific X-ray nanotomography, J. Am. Chem. Soc. 137 (2015) 102–105.
[7] Z. Liang, Z. Yin, H. Yang, Y. Xiao, W. Hang, J. Li, Nanoscale surface analysis that combines scanning probe microscopy and mass spectrometry: a critical review, TrAC Trends Anal. Chem. 75 (2016) 24–34.
[8] L. Quaroni, M. Obst, M. Nowak, F. Zobi, Three dimensional tomographic imaging of endogenous and exogenous molecules in a single intact cell with subcellular resolution, Angew. Chem. Int. Ed. 54 (2015) 318–322.
[9] Thermo Scientific XPS. Analysis Features. Monoatomic Depth Profiling, 2016 (Accessed 15 December 2016) http://xpssimplified.com/depth_profiling.php.
[10] M. Lépinay, D. Lee, R. Scarazzini, M. Bardet, M. Veillerot, M. Broussous, C. Licitra, V. Jousseaume, F. Bertin, V. Rouessac, A. Ayral, Impact of plasma reactive ion etching on low dielectric constant porous organosilicate films' microstructure and chemical composition, Microporous Mesoporous Mater. 228 (2016) 297–304.
[11] L.T. Canham (Ed.), Handbook of Porous Silicon, Springer International Publishing, Cham (ZG), Switzerland, 2014.
[12] N. Kumar, E. Froner, R. Guider, M. Scarpa, P. Bettotti, Investigation of non-specific signals in nanoporous flow-through and flow-over based sensors, Analyst 139 (2014) 1345–1349.
[13] T. Metke, A.S. Westover, R. Carter, L. Oakes, A. Douglas, C.L. Pint, Particulate-free porous silicon networks for efficient capacitive deionization water desalination, Sci. Rep. 6 (2016) 24680–24688.
[14] B. Xia, B. Wang, W. Zhang, J. Shi, High loading of doxorubicin into styrene-terminated porous silicon nanoparticles *via* π-stacking for cancer treatments *in vitro*, RSC Adv. 5 (2015) 44660–44665.

[15] M. Wang, P.S. Hartman, A. Loni, L.T. Canham, N. Bodiford, J.L. Coffer, Influence of surface chemistry on the release of an antibacterial drug from nanostructured porous silicon, Langmuir 31 (2015) 6179–6185.
[16] S. Näkki, J. Rytkönen, T. Nissinen, C. Florea, J. Riikonen, P. Ek, H. Zhang, H.A. Santos, A. Närvänen, W. Xu, V.P. Lehto, Improved stability and biocompatibility of nanostructured silicon drug carrier for intravenous administration, Acta Biomater. 13 (2015) 207–215.
[17] B. Fabre, Functionalization of oxide-Free silicon surfaces with redox-active assemblies, Chem. Rev. 116 (2016) 4808–4849.
[18] M.P. Stewart, J.M. Buriak, Photopatterned hydrosilylation on porous silicon, Angew. Chem. Int. Ed. 37 (1998) 3257–3260.
[19] E. Froner, R. Adamo, Z. Gaburro, B. Margesin, L. Pavesi, A. Rigo, M. Scarpa, Luminescence of porous silicon derived nanocrystals dispersed in water: dependence on initial porous silicon oxidation, J. Nanopart. Res. 8 (2006) 1071–1074.
[20] K.A. Kilian, T. Böcking, K. Gaus, J.J. Gooding, Introducing distinctly different chemical functionalities onto the internal and external surfaces of mesoporous materials, Angew. Chem. Int. Ed. 47 (2008) 2697–2699.
[21] C.-C. Wu, M.J. Sailor, Selective Functionalization of Internal and External surfaces of mesoporous silicon by liquid masking, ACS Nano 4 (2013) 3158–3167.
[22] W. Xu, J. Rytkönen, S. Rönkkö, T. Nissinen, T. Kinnunen, M. Suvanto, A. Närvänen, V.-P. Lehto, A nano-stopper approach to selectively engineer the surfaces of mesoporous silicon, Chem. Mater. 25 (2014) 6634–6742.
[23] P. Ashton, H. Guo, J. Chen, L.T. Canham, Porous silicon drug-eluting particles. US Patent 9,023,896, 2015.
[24] N. Daldosso, A. Ghafarinazari, P. Cortelletti, L. Marongiu, M. Donini, V. Paterlini, P. Bettotti, R. Guider, E. Froner, S. Dusi, M. Scarpa, Orange and blue luminescence emission to track functionalized porous silicon microparticles inside the cells of the human immune system, J. Mater. Chem. B 2 (2014) 6345–6353.
[25] Y. Ogata, H. Niki, T. Sakka, M. Iwasaki, Hydrogen in porous silicon: vibrational analysis of SiH_x species, J. Electrochem. Soc. 142 (1995) 195–201.
[26] R.M. Pasternack, A.S. Rivillon, Y.J. Chabal, Attachment of 3-(aminopropyl)triethoxysilane on silicon oxide surfaces: dependence on solution temperature, Langmuir 24 (2008) 12963–12971.
[27] N. Majoul, S. Aouida, B. Bessaïs, Progress of porous silicon APTES-functionalization by FTIR investigations, Appl. Surf. Sci. 331 (2015) 388–391.
[28] L. Wu, L. Cai, A. Liu, W. Wang, Y. Yuan, L. Zhanxiong, Self-assembled monolayers of perfluoroalkylsilane on plasma-hydroxylated silicon substrates, Appl. Surf. Sci. 349 (2015) 683–694.
[29] J.V. Tsybeskov, Blue emission in porous silicon: oxygen-related photoluminescence, Phys. Rev. B 49 (1994) 7821–7824.
[30] A. Halimaoui, Determination of the specific surface area of porous silicon from its etch rate in HF solutions, Surf. Sci. Lett. 306 (1994) L550–L554.
[31] Y. Chen, C. Zou, M. Mastalerz, S. Hu, C. Gasaway, X. Tao, Applications of micro-fourier transform infrared spectroscopy (FTIR) in the geological sciences-a review, Int. J. Mol. Sci. 16 (2015) 30223–30250.
[32] C.S. Fadley, R.J. Baird, W. Siekhaus, T. Novakov, S.A.L. Bergström, Surface analysis and angular distributions in x-ray photoelectron spectroscopy, J. Electron Spectrosc. Relat. Phenom. 4 (1974) 93–137.
[33] A. Jablonski, C.J. Powell, Relationships between electron inelastic mean free paths effective attenuation lengths, and mean escape depths, J. Electron Spectrosc. Relat. Phenom. 100 (1999) 137–160.
[34] J.R. Shallenberger, D.A. Cole, S.W. Novak, Characterization of silicon oxynitride thin films by x-ray photoelectron spectroscopy, J. Vacuum Sci. Technol. 17 (1999) 1086–1090.
[35] M. Haass, M. Darnon, O. Joubert, Sidewall passivation layer thickness and composition profiles of etched silicon patterns from angle resolved x-ray photoelectron spectroscopy analysis, J. Appl. Phys. 111 (2012) (124905-1 – 124905-6).
[36] J.F. Moulder, J. Chastain, Handbook of X-Ray Photoelectron Spectroscopy: A Reference Book of Standard Spectra for Identification and Interpretation of XPS Data, Perkin-Elmer Corporation, Physical Electronics Division, Eden Prairie MN, 1992.
[37] G. Dong-Jie, X. Shou-Jun, X. Bing, W. Shuai-, P. Jia, P. Yi, Y. Xiao-Zeng, G. Zhong-Ze, L. Zuhong, Reaction of porous silicon with both end-functionalized organic compounds bearing α-bromo and ω-carboxy groups for immobilization of biomolecules, J. Phys. Chem. B 109 (2005) 20620–20628.
[38] S.R. Puniredd, O. Assad, T. Stelzner, S. Christiansen, H. Haick, Catalyst-Free functionalization for versatile modification of nonoxidized silicon structures, Langmuir 27 (2011) 4764–4771.
[39] M. Haass, M. Darnon, O. Joubert, Sidewall passivation layer thickness and composition profiles of etched silicon patterns from angle resolved x-ray photoelectron spectroscopy analysis, J. Appl. Phys. 111 (2012) (124905-1-124905-6).
[40] G. Beamson, D. Briggs, High Resolution XPS of Organic Polymers. The Scienta ESCA300 Database, Wiley and Sons, Chichester, 1992.